

TRANSFORMS FOR RUNOFF AND SEDIMENT TRANSPORT

By Pierre Y. Julien,¹ Member, ASCE

ABSTRACT: Transforms reduce the distributions of surface-runoff and sediment-transport variables to near-exponential distributions typical of rainfall duration and intensity. Two transform parameters are determined from field measurements using either a graphical method or the method of moments. The transforms were tested on both small experimental plots and very large watersheds for the distributions of rainfall depth, runoff volume and discharge, sediment concentration and sediment discharge, as well as concentration and transport of chemicals from surface runoff. As expected from deterministic relationships, the inverse transform exponent \bar{b} for point rainfall is close to unity, increases to about 1.5 for runoff discharge, and varies between 1.5 and 3 for sediment and chemical transport. Several examples show that the transforms are useful to determine exceedance probability, flow and sediment duration curves, expected sediment load, and sediment-rating curves for poorly correlated concentration and discharge measurements.

INTRODUCTION

Soil detachment and chemical transport in upland areas is related to excess rainfall and surface runoff. The complexity of the physical processes between rainfall, surface runoff, sediment and chemical transport, not to mention the perturbations induced by human activities, contribute to make the problem of transport of sediment and chemicals a very difficult one to quantify. In general, the relationship between surface runoff and sediment or chemical transport is conducive to site-specific empirical formulas. The transport of fine sediments in terms of wash load and the transport of chemicals from surface runoff usually exhibit poor correlations with surface-runoff parameters such as flow depth, flow velocity, shear stress, or discharge. Coefficients of determination not exceeding 0.5 are commonly encountered, this causes difficulties in the determination of rainfall-sediment relationships from regression analysis. The need for correction factors [e.g., Ferguson (1986)] has been proposed to account for the large scatter of field measurements around the mean of log-transformed surface-runoff and transport variables.

There is extensive literature on extreme events and flood-frequency distributions that is to some extent germane to the foregoing analysis. Starting with Gumbel (1958), the contributions of Schaake et al. (1967), Todorovic (1968), Todorovic and Rousselle (1971), and Eagleson (1972, 1978) have been followed by Ashkar and Rousselle (1981), Hebson and Wood (1982), Diaz-Granados et al. (1984), Wood and Hebson (1986), Moughamian et al. (1987), Fontaine and Potter (1989), and Foufoula-Georgiou (1989). Most recent contributions include those of Shen et al. (1990), Cadavid et al. (1991), Kavvas and Govindaraju (1991), Govindaraju and Kavvas (1991), Hjelmfelt (1991), Hawkins (1993), and Raines and Valdes (1993).

This study is, however, not limited to extreme events and considers the entire database. In doing so, information will be quantified for the mean value, duration curves, and exceedance probability. Conceptually, this study stems from the probabilistic nature of rainfall parameters, which has been shown to compare very well with exponential probability density functions (EPDFs). Because runoff results from rainfall duration and intensity, an analysis based on the probability density function (PDF) of rainfall, runoff, and transport variables may

be preferable. The foregoing analysis expands upon the hypothesis that a power relationship exists between rainfall, runoff, and sediment variables (e.g., rainfall intensity and runoff discharge). This study attempts to determine the power relationship from an analysis of the PDFs of both variables.

The objective is to examine the properties of power transforms and their use in defining sediment-duration curves, the exceedance probability, and nonlinearities of rainfall-runoff-transport relationships from the plot size to large watersheds. This paper describes the transforms and tests the proposed procedure with field measurements of surface runoff and sediment and chemical transport at small and large scales. The method is summarized in terms of properties of rainfall characteristics, followed by the transform procedure and parameter evaluation. The findings from several applications to the PDF of runoff and transport variables lead to a discussion of the nonlinearity of rainfall-runoff-transport relationships.

RAINFALL CHARACTERISTICS

Rainfall characteristics are important because they generate surface runoff and transport of sediment and chemicals. Point-rainfall precipitation can be described as a random time series of discrete storm events, each event having finite duration and constant intensity. Several stochastic models have been developed since Todorovic (1968) and Todorovic and Woolhiser (1974). In these models, rainfall precipitation has been described as a Poisson arrival process of rainfall events of duration t_r and average rainfall intensity i .

The storm duration t_r has been found to be exponentially distributed. Considering a period where the average rainfall duration \bar{t}_r remains constant, the PDF of the storm duration $p(t_r)$ is given by

$$p(t_r) = \lambda_1 e^{-\lambda_1 t_r} \quad (1)$$

in which the rainfall duration parameter $\lambda_1 = 1/\bar{t}_r$ is the reciprocal of the average storm duration \bar{t}_r .

The rainstorm intensity i has also been shown to be exponentially distributed. The probability density function, $p(i)$, is

$$p(i) = \lambda_2 e^{-\lambda_2 i} \quad (2)$$

in which the rainfall intensity parameter $\lambda_2 = 1/\bar{i}$ is the reciprocal of the average rainstorm intensity \bar{i} . Good agreement between the EPDF for both rainfall duration and intensity were reported in the literature by Eagleson (1978), and on a monthly basis by Nguyen and Rousselle (1981) and Julien (1982). Julien and Frenette (1985) examined the monthly variability in expected rainfall erosion from the monthly variability in average rainfall duration and intensity.

¹Prof. of Civ. Engrg., Engrg. Res. Ctr., Colorado State Univ., Fort Collins, CO 80523.

Note. Discussion open until December 1, 1996. To extend the closing date one month, a written request must be filed with the ASCE Manager of Journals. The manuscript for this paper was submitted for review and possible publication on September 11, 1995. This paper is part of the *Journal of Hydrologic Engineering*, Vol. 1, No. 3, July, 1996. ©ASCE, ISSN 1084-0699/96/0003-0114-0122/\$4.00 + \$.50 per page. Paper No. 11601.

TRANSFORMS

The details of the proposed transforms are presented with emphasis on the procedure and on the evaluation of the transform parameters. Properties of an EPDF of variable y are such that after dividing the variable y by the mean value \bar{y} , a reduced variable ϕ is defined as $\phi = y/\bar{y}$. The properties of the EPDF $p(\phi)$ and the exceedance probability $P(\phi)$ defined as $P(\phi) = \int_{\phi}^{\infty} p(\phi) d\phi$ are such that

$$P(\phi) = p(\phi) = e^{-\phi} \quad (3)$$

The identity between both the EPDF and the exceedance probability will yield useful applications.

The purpose of the transform is to determine whether the PDF of a runoff or sediment variable x reduces to an EPDF of variable ϕ after the following transform:

$$\phi = ax^b \quad (4)$$

where a and b = transform coefficient and exponent, respectively, hereby referred to as transform parameters. If successful, this would transform the unknown exceedance probability of variable x into a simple EPDF of the reduced variable ϕ .

The inverse transform is simply defined from (4) as

$$x = (1/a)^{1/b} \phi^{1/b} = \hat{a}\phi^{\hat{b}} \quad (5)$$

where \hat{a} and \hat{b} = inverse transform parameters simply calculated from a and b as $\hat{a} = (1/a)^{1/b}$ and $\hat{b} = 1/b$. Conversely, one finds $a = \hat{a}^{-1/\hat{b}} = \hat{a}^{-b}$ and $b = 1/\hat{b}$. The inverse transform exponent \hat{b} is most important to determine the degree of nonlinearity of the variable x and can be related to deterministic relationships.

The properties of the transform are such that once the transform parameters a and b are known, the exceedance probability of variable x is calculated directly from (3) and (4). The PDF $p(x)$ is a Weibull distribution

$$p(x) = abx^{b-1}e^{-ax^b} = ab(\phi/a)^{(b-1)/b}e^{-\phi} \quad (6)$$

One can also demonstrate that $p(x) dx = p(\phi) d\phi$ and $P(x) = P(\phi)$. Stedinger et al. (1993) cites relationships between the Weibull, Gumbel, and generalized extreme value distributions. For instance, if x has a Weibull distribution, $y = -\ln x$ has a Gumbel distribution and the goodness-of-fit tests available for the Gumbel can be applied to the Weibull distribution. The emphasis of this study is to define the transform parameters a and b in order to take advantage of the properties of the exponential distribution for ϕ .

TRANSFORM PARAMETER EVALUATION

Two procedures are examined for the transform parameter evaluation: a graphical method; and the method of moments. A detailed example of the evaluation procedure follows. It may be noted that Gumbel (1958) approached a similar problem with the maximum-likelihood method but needed successive approximations for the solution.

Graphical Method

The graphical method capitalizes on the properties of the EPDF and exceedance probability in (3). The natural logarithm of (3) is combined with (4) to give

$$-\ln P(\phi) = \phi = ax^b \quad (7)$$

The transform parameters a and b will be evaluated graphically after taking the natural logarithm of (7) in the form

$$\Pi = \ln(-\ln P) = \ln[-\ln P(\phi)] = \ln \phi = \ln a + b \ln x \quad (8)$$

where the shorthand exceedance probability Π designates the

double logarithm of the exceedance probability P . Of course, this transform requires all values of x to be positive.

A straight line is fitted on the graphical presentation of Π as a function of $\ln x$ to yield estimates for a and b . It becomes clear from (8) that $\ln a$ corresponds to the value of Π when $x = 1$. Likewise, if the points on the graph Π versus $\ln x$ assemble on a straight line, the slope of the line gives directly the transform exponent b . The graphical method is subjective but provides a qualitative appreciation of the goodness of fit. Ideally, all points should plot on a straight line for the power transform in (4) to be exactly applicable.

Method of Moments

Parameter estimation from the method of moments takes advantage of the information contained in the first and second moments of the sample. The transform parameters a and b can be evaluated after equating with the first and second moments of the transformed variables. Specifically, the first moment, or mean value, of the sample \bar{x} is equated to the first moment M_1 of the transformed distribution, given $x = (\phi/a)^{1/b}$ and $p(x) dx = p(\phi) d\phi$

$$M_1 = \int_0^{\infty} xp(x) dx = \left(\frac{1}{a}\right)^{1/b} \int_0^{\infty} \phi^{1/b} e^{-\phi} d\phi = \left(\frac{1}{a}\right)^{1/b} \Gamma\left(1 + \frac{1}{b}\right) = \hat{a}\hat{b} = \bar{x} \quad (9)$$

TABLE 1. Useful Values of Transform Parameter b

| b (1) | \bar{x}^2/\bar{x}^2 (2) | $\Gamma(b)$ (3) | $!(b)$ (4) |
|------------|------------------------------|--------------------|---------------|
| 0.1 | 184,756 | 9.51 | 0.951 |
| 0.15 | 2,213 | 6.22 | 0.933 |
| 0.2 | 252 | 4.59 | 0.918 |
| 0.25 | 70 | 3.62 | 0.906 |
| 0.3 | 30.243 | 2.99 | 0.897 |
| 0.35 | 16.777 | 2.54 | 0.891 |
| 0.4 | 10.864 | 2.21 | 0.887 |
| 0.45 | 7.793 | 1.97 | 0.886 |
| 0.5 | 6 | 1.77 | 0.886 |
| 0.55 | 4.861 | 1.61 | 0.888 |
| 0.6 | 4.090 | 1.49 | 0.893 |
| 0.65 | 3.543 | 1.38 | 0.900 |
| 0.7 | 3.138 | 1.30 | 0.908 |
| 0.75 | 2.830 | 1.22 | 0.919 |
| 0.8 | 2.588 | 1.16 | 0.931 |
| 0.85 | 2.395 | 1.11 | 0.945 |
| 0.9 | 2.238 | 1.07 | 0.962 |
| 0.95 | 2.108 | 1.02 | 0.980 |
| 1 | 2 | 1.00 | 1.00 |
| 1.05 | 1.907 | 0.973 | 1.02 |
| 1.1 | 1.828 | 0.951 | 1.046 |
| 1.2 | 1.700 | 0.918 | 1.10 |
| 1.3 | 1.601 | 0.897 | 1.17 |
| 1.4 | 1.523 | 0.887 | 1.24 |
| 1.5 | 1.460 | 0.886 | 1.33 |
| 1.6 | 1.409 | 0.893 | 1.43 |
| 1.7 | 1.366 | 0.909 | 1.54 |
| 1.8 | 1.330 | 0.931 | 1.68 |
| 1.9 | 1.299 | 0.962 | 1.83 |
| 2 | 1.273 | 1.00 | 2.0 |
| 2.5 | 1.183 | 1.33 | 3.32 |
| 3 | 1.132 | 2.0 | 6.0 |
| 3.5 | 1.100 | 3.32 | 11.6 |
| 4 | 1.078 | 6.0 | 24.0 |
| 4.5 | 1.063 | 11.6 | 52.3 |
| 5 | 1.052 | 24 | 120 |
| 6 | 1.037 | 120 | 720 |
| 7 | 1.028 | 720 | 5,040 |
| 8 | 1.022 | 5,040 | 40,320 |
| 9 | 1.017 | 40,320 | 362,880 |
| 10 | 1.014 | 362,880 | 3,628,800 |

Accordingly, the expected value \bar{x} can be simply evaluated from a simple gamma function of the inverse transform parameters as $\bar{x} = a!b$, where ! designates the factorial function of the argument \hat{b} .

Likewise, the second moment of the sample \bar{x}^2 is equated to the second moment M_2 of the transformed distribution

$$M_2 = \int_0^{\infty} x^2 p(x) dx = \left(\frac{1}{a}\right)^{2b} \int_0^{\infty} \phi^{2b} e^{-\phi} d\phi$$

$$= \left(\frac{1}{a}\right)^{2b} \Gamma\left(1 + \frac{2}{b}\right) = a^2!(2\hat{b}) = \bar{x}^2 \quad (10)$$

The evaluation of the transform parameters a and b follows after the transform coefficient a is eliminated from the ratio (10) to the square of (9), thus

$$\frac{\bar{x}^2}{\bar{x}^2} = \frac{\Gamma\left(1 + \frac{2}{b}\right)}{\left[\Gamma\left(1 + \frac{1}{b}\right)\right]^2} = \frac{!(2\hat{b})}{[!\hat{b}]^2} \quad (11)$$

From the calculated values of \bar{x} and \bar{x}^2 of the sample, the value of b on the right-hand side of (11) can best be evaluated numerically. For instance, an interpolation procedure based on the numerical values given in Table 1 proves to be sufficiently accurate. The value of the transform coefficient a then follows from $a!b = \bar{x}$ in (9) as

$$a = \left[\frac{\Gamma\left(1 + \frac{1}{b}\right)}{\bar{x}} \right]^b = \left[\frac{!\hat{b}}{\bar{x}} \right]^{1/\hat{b}} \quad (12)$$

Parameter estimation from the method of moments is direct and not subjective but lacks the visual information inherent to the graphical method. The evaluation of the transform parameters using both the graphical method and the method of moments is illustrated with the following example.

PARAMETER-EVALUATION EXAMPLE

Consider the following sample of an unknown variable $\tilde{x} = 4.5, 1.0, 7.0, 2.0, 9.0, 0.5, 6.0, 11.0,$ and 3.5 . The first step consists of ranking the $n = 9$ numbers in decreasing order of x as shown in Table 2, column 2; the values of x are squared in column 3. The second step consists of calculating the exceedance probability using the Weibull plotting position. Accordingly, the numbers in decreasing order are ranked from 1 to n as shown in column 4; 1 being the largest and n being the smallest number. After dividing the rank by $1 + n$, the plotting position corresponds to the exceedance probability $P(\phi)$ or $P(x)$ in column 5. The values of $\ln x$ and $\Pi = \ln[-\ln P(\phi)]$ are tabulated in columns 6 and 7, respectively, for the plot shown in Fig. 1. Graphically, the parameter estimation gives $a \approx 0.1$ and $b \approx 1.3$. The line is usually fit through the higher values of $\ln x$ because for sediment-transport parameters the large values of x are usually those contributing to most of the sediment load.

Using the method of moments, the average value, $\bar{x} = 4.94$ is calculated at the bottom of Table 2, column 2. The average value of $\bar{x}^2 = 36.1$ is compiled at the bottom of column 3. From Table 1, the ratio $\bar{x}^2/\bar{x}^2 = 36.1/(4.94)^2 = 1.479$ in column 2 corresponds to a value of $b \approx 1.45$ from interpolation with the values given in Table 1, column 1. The value of $a \approx 0.085$ is thereafter calculated from (12). We note that the gamma function can be approximated by Stirling's asymptotic series

TABLE 2. Example of Transformation Procedure

| Sample \tilde{x} (1) | Ranked x (2) | x^2 (3) | Rank (4) | $P(x)$ (5) | $\ln(x)$ (6) | $\ln[-\ln P(x)]$ (7) |
|---------------------------|-------------------|--------------------|-------------|---------------|-----------------|-------------------------|
| 4.5 | 11.0 | 121.00 | 1 | 0.1 | 2.3979 | 0.8340 |
| 1.0 | 9.0 | 81.00 | 2 | 0.2 | 2.1972 | 0.4759 |
| 7.0 | 7.0 | 49.00 | 3 | 0.3 | 1.9459 | 0.1856 |
| 2.0 | 6.0 | 36.00 | 4 | 0.4 | 1.7918 | -0.0874 |
| 9.0 | 4.5 | 20.25 | 5 | 0.5 | 1.5041 | -0.3665 |
| 0.5 | 3.5 | 12.25 | 6 | 0.6 | 1.2528 | -0.6717 |
| 6.0 | 2.0 | 4.00 | 7 | 0.7 | 0.6931 | -1.0309 |
| 11.0 | 1.0 | 1.00 | 8 | 0.8 | 0.0000 | -1.4999 |
| 3.5 | 0.5 | 0.25 | 9 | 0.9 | -0.6931 | -2.2504 |
| Average | $\bar{x} = 4.94$ | $\bar{x}^2 = 36.1$ | — | — | — | — |

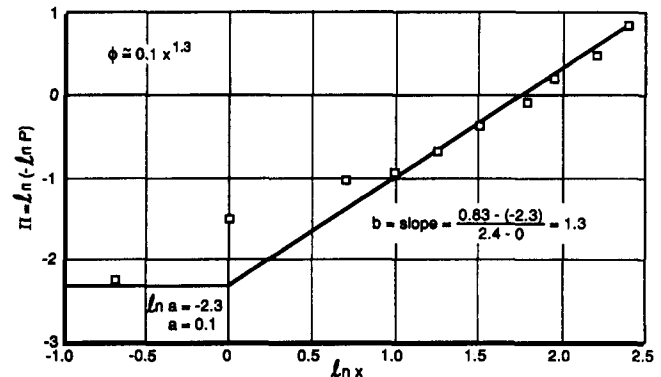


FIG. 1. Example of Transform Parameter Evaluation

$$!(x) = \Gamma(x + 1)$$

$$= \sqrt{2\pi x} x^x e^{-x} \left\{ 1 + \frac{1}{12x} + \frac{1}{288x^2} - \frac{139}{51840x^3} \dots \right\} \quad (13)$$

which is sufficiently accurate when $x > 0.25$.

TRANSFORMS FOR SURFACE RUNOFF AND SEDIMENT TRANSPORT

Excess rainfall generates surface runoff as overland flow and channel flow. To capture the essential features of the rainfall-runoff relationship, a rectangular hyetograph of constant excess rainfall intensity i and duration t_r is considered. An important parameter in surface-runoff modeling is the resistance relationship, which can be written as $q = \alpha h^\beta$, where the unit discharge q is a power function of flow depth h . The resistance coefficients are found in Table 3 in terms of Darcy-Weisbach friction factor f , Chézy coefficient C , Manning n , or laminar resistance coefficient K for various overland flow conditions including friction slope S , runoff length L , gravitational acceleration g , and kinematic fluid viscosity ν . Woolhiser (1975) presented a method to evaluate resistance coefficients in overland flow.

The time to equilibrium t_e is defined as the time at which the surface runoff reaches an equilibrium state. On a rectangular plane, it is calculated when flow depth $h = it_e$ is sufficiently large to convey the equilibrium discharge $q = \alpha h^\beta = iL$. The general solution for t_e is a function of the flow-resistance relationship and excess rainfall intensity i

$$t_e = \left[\frac{L}{\alpha i^{\beta-1}} \right]^{1/\beta} \quad (14)$$

Values of t_e for different resistance relationships are presented in Table 3. Surface runoff from the dimensional equations of Woolhiser (1977) over a rectangular plane of length L can be written in dimensionless form $\psi = q/(iL)$ as a function of the dimensionless time $\theta = (t - t_r)/t_e$, where t_e = time to equilib-

TABLE 3. Resistance Relationships $q = \alpha h^\beta$

| Flow type (1) | Resistance coefficient (2) | α (3) | β (4) | t_e (5) |
|------------------|-------------------------------|-----------------|----------------|------------------------------|
| Laminar | $K = \text{constant}$ | $8gS/Kv$ | 3 | $(KvL/8gSi^2)^{1/3}$ |
| Turbulent | | | | |
| Darcy-Weisbach | $f = \text{constant}$ | $\sqrt{8gS/f}$ | 1.5 | $(fL^2/8gSi)^{1/3}$ |
| Chézy | $C = \text{constant}$ | $CS^{1/2}$ | 1.5 | $(L^2/C^2Si)^{1/3}$ |
| Manning (S.I.) | $n = \text{constant}$ | $S^{1/2}/n$ | 1.67 | $(nL/S^{1/2})^{0.667}^{0.6}$ |

rium. Fig. 2 illustrates the shape of dimensionless surface-runoff hydrographs on rectangular planes. The general dimensionless relationships for the rising and falling limbs in the ψ - θ plane are valid for any resistance equation.

In the case of small watersheds, surface runoff is essentially described by complete equilibrium hydrographs. Complete equilibrium hydrographs are those for which the rainfall duration t_r exceeds the time to equilibrium t_e , hence the dimensionless ratio $\lambda = t_r/t_e$ is greater than unity. The surface runoff hydrograph can be subdivided into three parts: rising limb, equilibrium, and falling limb. The rising limb of the complete equilibrium hydrograph is given by $\psi = (\theta + \lambda)^\beta$. The equilibrium discharge simply equals $\psi = 1$, and the falling limb is given by $\theta = (1 - \psi)/\beta\psi^{(\beta-1)/\beta}$, as shown in Fig. 2. Given constant excess rainfall intensity, Julien and Moglen (1990), Ogden and Julien (1993), Saghafian et al. (1995), and Ogden et al. (1995) highlighted similarities in surface-runoff characteristics between one-dimensional planes and two-dimensional surface-runoff hydrographs. Essentially, small watersheds are characterized with values of $\lambda = t_r/t_e > 1$ for which the dimensionless discharge during the equilibrium portion of the hydrograph is close to unity. Accordingly, the magnitude of the maximum discharge varies linearly with the rainfall intensity, $\psi = iL$. Consequently, the PDF of surface runoff and the PDF of discharge measurements should closely approximate the PDF of rainfall intensity. For near impervious small watersheds, one therefore expects the exponent b of the transforms to remain close to unity, resulting in a near EPDF for runoff discharge.

Sediment transport from small watersheds is known to vary with rainfall intensity but also depends largely on infiltration (e.g., there is little sediment transport when the infiltration rate exceeds the rainfall intensity). Surface runoff is usually a better parameter to correlate with sediment transport than rainfall. For instance, the power relationship $q_s \sim q^d$ for surface runoff gives empirical values of the exponent $1.4 < d < 2.4$ [e.g., Julien (1995), p. 223]. Accordingly, the inverse transform parameter for sediment and perhaps chemical transport from small watersheds is expected to be $1.5 < \hat{b} < 2.5$ if the rainfall-runoff relationship is nearly linear.

Large watersheds are hereby referred to those with time to equilibrium t_e exceeding the duration of rainfall t_r , or $\lambda = t_r/t_e < 1$. With reference to Fig. 2, the hydrograph is said to reach partial equilibrium characterized with low peak discharge at an amplitude corresponding to $\psi = \lambda^\beta < 1$, or $q < iL$. From this relationship, one infers that the maximum discharge under partial equilibrium is $q \cong iL(t_r/t_e)^\beta$. In statistical terms, on a watershed with given topography in constant α and constant L , considering t_e from (14), the PDF of maximum unit discharge depends on the PDF of $i^{2-(1/\beta)}t_r^\beta$. As opposed to the results from small watersheds, the PDF of surface-runoff discharge on large watersheds should therefore reflect the resistance equation through β , which should be somewhat comparable to the inverse transform exponent \hat{b} , or approximately $1 < \hat{b} < \beta$ when i and t_r are independent.

Sediment transport from large watersheds should become difficult to quantify because of the nonlinearity of the rainfall-

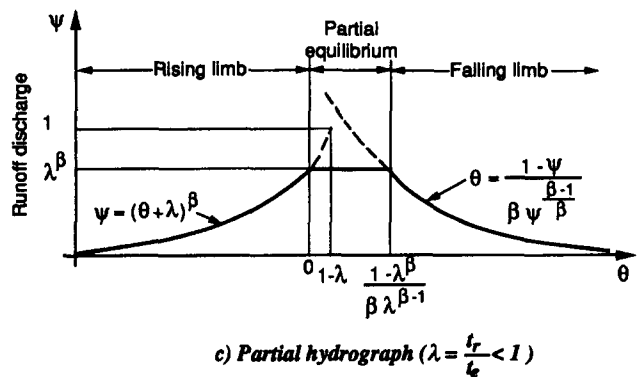
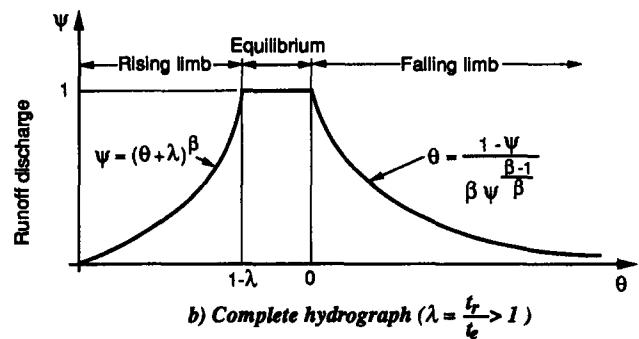
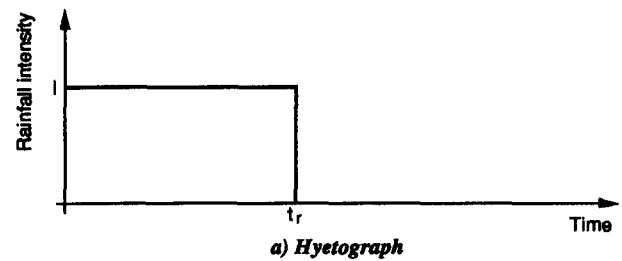


FIG. 2. Hyetograph, Complete, and Partial Equilibrium Hydrographs for Rectangular Planes

runoff relationship. However, one may expect a higher inverse transform parameter, $\hat{b} > 1.5$, for sediment discharge in large rivers.

APPLICATIONS TO SMALL WATERSHEDS

Point Rainfall

The analysis of natural point-rainfall processes serves as the generating function for the surface-runoff and sediment-transport processes. As previously explained, the PDF of rainfall duration and rainfall intensity have been demonstrated to be near-exponentially distributed and independent. The meteorological data from the agronomic station at Laval University, near Québec City, Canada, has been used for the analysis of the PDF of rainfall duration. Measurements with an accuracy of ± 5 min were available (Villeneuve 1968) during the months of June–November from 1966 to 1970. The values of the transform parameters are given in Table 4 as calculated from both the graphical method and the method of moments. The results of both methods confirm that the transform exponent b remains close to unity. The linearity of the transformed distribution is very good as shown in Fig. 3.

The PDF of rainfall depth from individual rainstorms has been examined with the Laval University data collected during June–November 1966–1970 with an accuracy of ± 0.01 in. The transform for rainfall depth is given in Table 4 for comparison with other processes. The inverse transform exponent, $\hat{b} \cong 1.2$, differs slightly from unity but the transformed distributions of rainfall depth fits a straight line as shown in Fig.

TABLE 4. Typical Values of Transform Parameters

| Variable (1) | Unit (2) | Watershed size (3) | Location (4) | Number of points (5) | INVERSE TRANSFORMS $x = \hat{a}\hat{b}$ | | | | TRANSFORMS $\phi = ax^b$ | | | |
|----------------------------|----------------------|--------------------------|-----------------|----------------------------|--|------------------|------------------|------------------|-----------------------------|-------------|-----------------------|-------------|
| | | | | | Graphical | | Moments | | Graphical | | Moments | |
| | | | | | \hat{a} (6) | \hat{b} (7) | \hat{a} (8) | \hat{b} (9) | a (10) | b (11) | a (12) | b (13) |
| (a) Rainfall | | | | | | | | | | | | |
| Duration (t_r) | min. | point | Quebec | 327 | 263 | 1.08 | 257 | 1.02 | 5.87×10^{-3} | 0.92 | 4.32×10^{-3} | 0.98 |
| Depth (i_r) | in. | point | Quebec | 327 | 0.29 | 1.28 | 0.29 | 1.21 | 2.63 | 0.78 | 2.77 | 0.82 |
| Depth (i_r) | in. | plot 1 | Missouri | 402 | 1.10 | 1.03 | 1.27 | 0.90 | 0.87 | 0.97 | 0.77 | 1.10 |
| Depth (i_r) | in. | plot 3 | Missouri | 410 | 1.18 | 0.94 | 1.31 | 0.85 | 0.84 | 1.06 | 0.73 | 1.18 |
| (b) Snowmelt | | | | | | | | | | | | |
| Discharge | mL/s | plot | Quebec | 389 | 8.46 | 1.37 | 9.92 | 1.15 | 0.21 | 0.73 | 0.14 | 0.87 |
| (c) Runoff | | | | | | | | | | | | |
| Volume/area | in. | plot 1 | Missouri | 404 | 0.32 | 1.52 | 0.31 | 1.62 | 2.11 | 0.66 | 2.06 | 0.62 |
| Volume/area | in. | plot 33 | Missouri | 438 | 0.34 | 1.46 | 0.35 | 1.47 | 2.08 | 0.68 | 2.06 | 0.68 |
| Discharge | m ³ /s | 5,830 km ² | Quebec | 3,285 | 82.8 | 1.77 | 98.4 | 1.52 | 0.083 | 0.56 | 0.048 | 0.66 |
| Discharge | ft ³ /sec | 279,460 km ² | Colorado River | 1,826 | 9,557 | 1.62 | 12,931 | 1.25 | 3.5×10^{-3} | 0.62 | 5.25×10^{-4} | 0.80 |
| (d) Chemical Concentration | | | | | | | | | | | | |
| Ammonia | ppm | 50 km ² | Iowa | 1,005 | 0.26 | 1.34 | 0.27 | 1.41 | 2.67 | 0.75 | 2.51 | 0.71 |
| Nitrate | ppm | 50 km ² | Iowa | 1,094 | 8.91 | 0.46 | 7.56 | 0.67 | 8.8×10^{-3} | 2.16 | 0.05 | 1.47 |
| Orthophosphate | ppm | 50 km ² | Iowa | 1,104 | 0.05 | 1.48 | 0.057 | 1.40 | 7.5 | 0.67 | 7.6 | 0.71 |
| (e) Chemical Yield | | | | | | | | | | | | |
| Nitrate | lb/acre | plot 33 | Missouri | 187 | 0.11 | 1.63 | 0.08 | 2.22 | 3.77 | 0.61 | 3.05 | 0.45 |
| Ammonia | lb/acre | plot 33 | Missouri | 185 | 0.027 | 2.33 | 0.032 | 2.25 | 4.72 | 0.43 | 4.61 | 0.44 |
| Orthophosphate | lb/acre | plot 33 | Missouri | 165 | 0.014 | 1.81 | 0.017 | 1.48 | 10.5 | 0.55 | 15.4 | 0.67 |
| Sediment nitrogen | lb/acre | plot 33 | Missouri | 159 | 0.93 | 2.13 | 1.08 | 2.09 | 1.04 | 0.47 | 0.96 | 0.47 |
| Sediment phosphate | lb/acre | plot 33 | Missouri | 117 | 0.019 | 2.22 | 0.022 | 2.16 | 5.91 | 0.45 | 5.81 | 0.46 |
| (f) Sediment | | | | | | | | | | | | |
| Concentration | mg/L | 5,830 km ² | Quebec | 1,377 | 30.0 | 1.64 | 20.8 | 2.14 | 0.13 | 0.61 | 0.24 | 0.47 |
| Concentration | mg/L | 279,460 km ² | Colorado River | 1,826 | 3,016 | 1.26 | 3,362 | 1.13 | 1.74×10^{-3} | 0.79 | 7.5×10^{-4} | 0.88 |
| Yield | t/acre | plot 33 | Missouri | 284 | 0.23 | 2.35 | 0.25 | 2.20 | 1.86 | 0.42 | 1.89 | 0.45 |
| Discharge (Q_r) | t/day | 5,830 km ² | Quebec | 1,375 | 392 | 2.84 | 493 | 2.56 | 0.12 | 0.35 | 0.089 | 0.39 |
| Discharge (Q_r) | t/day | 279,460 km ² | Colorado River | 1,826 | 79,875 | 2.18 | 120,230 | 1.70 | 5.74×10^{-3} | 0.46 | 1.04×10^{-3} | 0.59 |

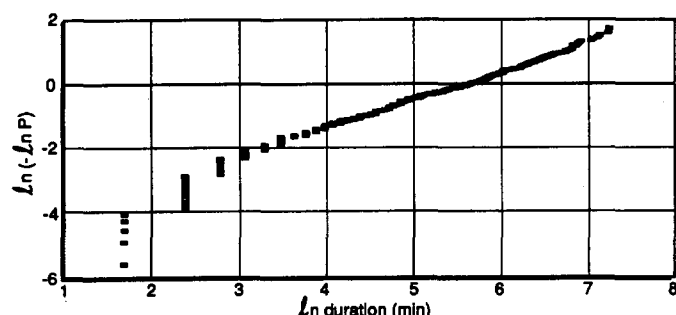


FIG. 3. Transform Diagram for Point Rainfall Duration

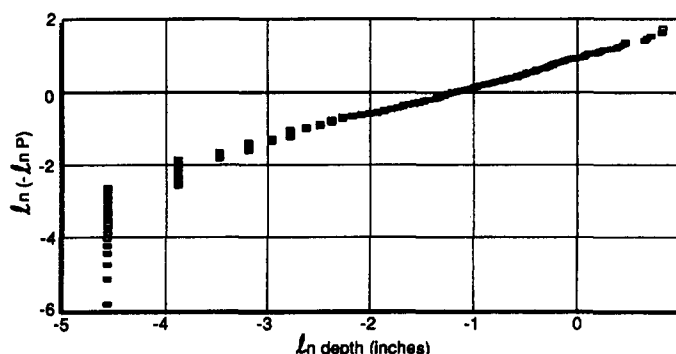


FIG. 4. Transform Diagram for Point Rainfall Depth

4. The rainfall precipitation measurements on claypan soils at Kingdom City, Missouri (R. B. Burwell, unpublished USDA ARS Watershed Research Unit report, 1982; Hjelmfelt and Burwell 1984; Jamison et al. 1968) were considered for comparison. The precipitation depth measurements give transform exponents close to unity for plots 1 and 33, as shown in Table 4.

Surface Runoff on Small Plots

The surface-runoff volume from a single event is usually expected to be less than the volume of rainfall. Indeed, in previous small watersheds, surface runoff is generated from the rainfall intensity in excess of the infiltration rate. The precipitation measurements of the claypan soils in Missouri (Burwell, unpublished report, 1982) were examined in terms of the

relationship between rainfall depth and surface-runoff depth. At rainfall depths not exceeding 2.5 cm (1 in.), the surface-runoff depth is almost negligible. Conversely, as the rainfall precipitation depth approaches 25 cm (10 in.), the surface-runoff depth becomes asymptotically equal to the rainfall depth. The proposed transforms are used to reduce the runoff depth data into an EPDF as shown in Fig. 5. The transform parameters are compiled in Table 4 for comparison with other precipitation variables.

Finally, the PDF of snowmelt has been examined with the proposed transforms; specifically, the hourly snowmelt data of Rousseau (1979) has been processed for comparison with other precipitation variables. Although the time variability of hourly snowmelt data is highly nonlinear (Julien 1982), the

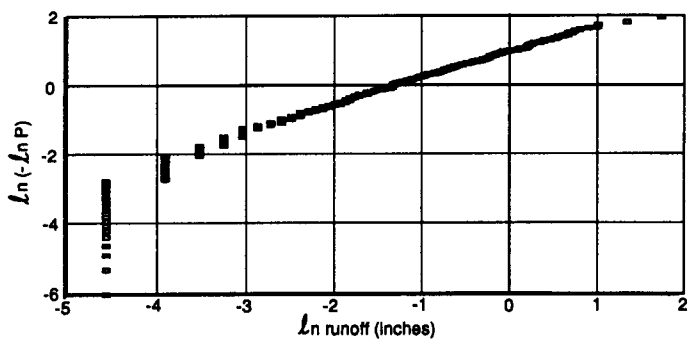


FIG. 5. Transform Diagram for Runoff Volume per Surface Area

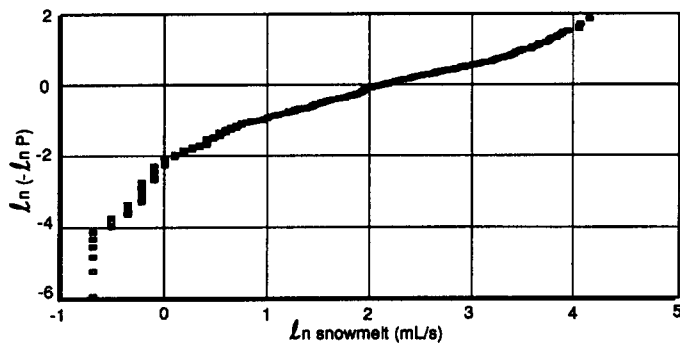


FIG. 6. Transform Diagram for Hourly Snowmelt Discharge

transforms of the data set covering an entire snowmelt season indicate a fairly linear fit of the reduced variable as shown in Fig. 6. The results in Table 4 are quite comparable to those for rainfall intensity.

Sediment and Chemical Transport

Sediment and chemical transport from small watersheds is intriguing given the poor correlation between sediment, or chemical concentration, with rainfall parameters. The use of the proposed transforms is first demonstrated in terms of concentration. The data collected at Four Mile Creek, Iowa, during the period 1976–78 (Johnson and Baker 1982) has been examined for this analysis. Similar results were obtained for the transport of agricultural chemicals from small upland watersheds near Watkinsville, Georgia (Smith et al. 1978). As shown in Table 4, the transforms yield reasonable agreement between the measured concentrations of ammonia and orthophosphate, while the values of the inverse transform exponents \hat{b} range between 1.34 and 1.48. The concentration of nitrate yields ambiguous results because both surface and subsurface flows contribute to the concentration. Fig. 7 is quite typical of the PDF in chemical concentration yielded from agricultural plots as viewed from the proposed transforms.

In terms of sediment yield, the PDF of the sediment delivery from experimental plots is subjected to poor correlation with either rainfall depth or surface-runoff depth. Nevertheless, the proposed transforms reduce the sediment yield data from the claypan soils in Missouri into valuable results shown in Fig. 8. The inverse transform exponents are listed in Table 4, and, the sediment yield corresponds to a higher power of the rainfall or runoff parameter. As expected in sediment-transport studies, the sediment discharge varies with approximately the square of the water discharge. This is reflected in the inverse transform exponents $\hat{b} > 2$ for sediment yield in Table 4.

The delivery of chemicals from agricultural plots of the claypan soils in Missouri was examined to determine the transform parameters listed in Table 4, which are quite consistent for all five chemicals measured: nitrate, sediment nitrogen, ammonia, sediment phosphate, and orthophosphate. The yield of

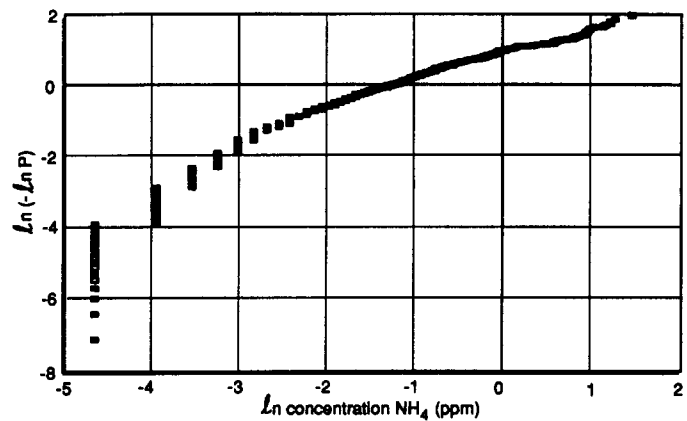


FIG. 7. Transform Diagram for Ammonium Concentration from Small Watershed

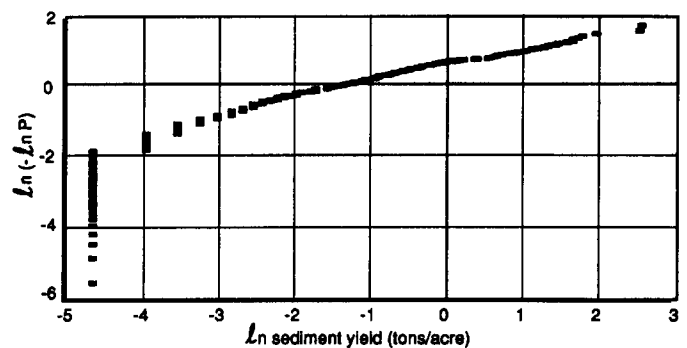


FIG. 8. Transform Diagram for Sediment Yield from Small Watershed

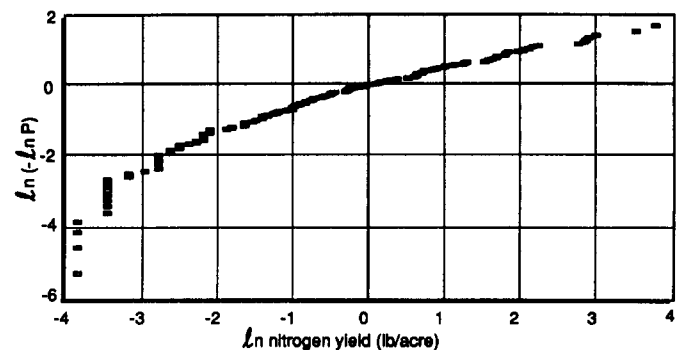


FIG. 9. Transform Diagram for Nitrogen Yield from Small Watershed

chemicals from agricultural plots varies roughly with the second power of the linear rainfall processes; Fig. 9 is quite typical of the results.

APPLICATIONS TO LARGE WATERSHEDS

The application to large watersheds focuses on the PDF of daily discharges, sediment concentration, and sediment discharge. Two large watersheds were considered: the Chaudière river in Canada covers 5,830 km² and was sampled during 1968–76; and the Colorado river at Lee's Ferry in Arizona covers 279,460 km² and was sampled daily from 1955 to 1959. Daily discharge measurements from the Chaudière river provide the flow-duration curve in terms of transform diagram in Fig. 10, which exhibits a nearly straight fit of the transformed distribution at higher discharges. The values of the inverse transform exponent $1.52 < \hat{b} < 1.77$ are quite comparable to the resistance exponent $1.5 < \beta < 1.67$ in Table 3 for turbulent flow.

As a first application example, the transforms provide useful

information in the analysis of exceedance probability and flow duration curves. Indeed, the exceedance probability of a discharge Q can be directly calculated from (3) and (4)

$$P(x) = e^{-ax^b} = e^{-(x/d)^{1/b}} \quad (15)$$

given the transform parameters in Table 4. For instance, the flow discharge in the Chaudière river is given by $\phi = 0.048Q^{0.66}$ from Table 4. The exceedance probability $P(1,000 \text{ m}^3/\text{s})$ of a daily discharge $Q = 1,000 \text{ m}^3/\text{s}$ is approximately $P(1,000) \equiv e^{[-0.048 \cdot 1,000^{0.66}]} = 0.01$, which compares well with the recorded value (0.008) on the flow-duration curve reported in Julien (1995, p. 234). Actually, the entire flow-duration curve for this river is in very good agreement with (15).

Sediment concentration was measured periodically with emphasis during the periods of high discharge. The upper portion of the concentration diagram (Fig. 11) is also quite amenable to the use of the proposed transforms, for which the exceedance probability of sediment concentration can be calculated from (15). From the relationship in Table 4 the inverse transform exponent $1 < \hat{b} < 2$ indicates that sediment concentration varies nonlinearly with the exponential rainfall characteristics.

As a second example, the sediment-rating curve during the

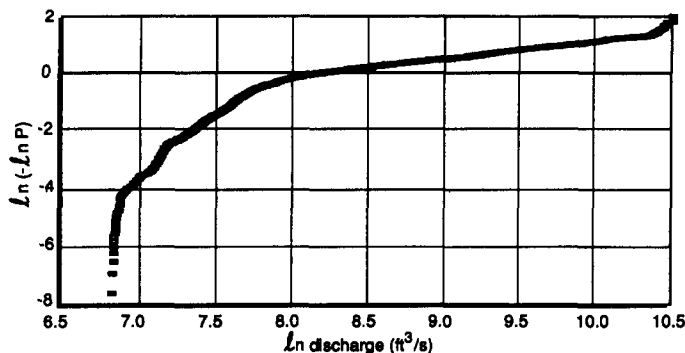


FIG. 10. Transform Diagram for Daily Discharge from Chaudière River

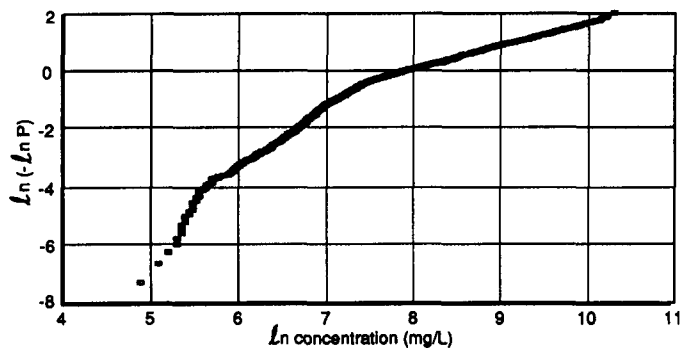


FIG. 11. Transform Diagram for Sediment Concentration in Chaudière River

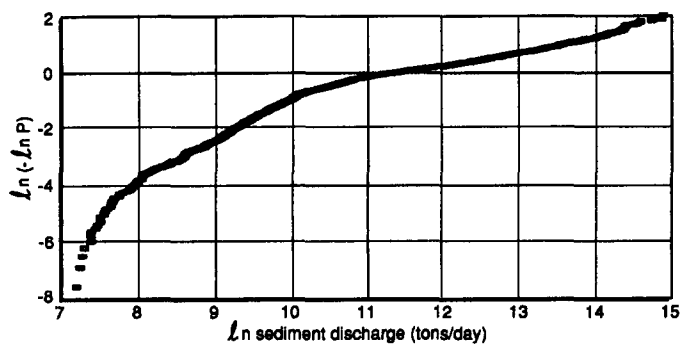


FIG. 12. Transform Diagram for Daily Sediment Discharge in Colorado River

period of sampling can also be examined with the use of the transforms. From the method of moments in Table 4, the transform of sediment concentration for the Chaudière river is $\phi = 0.24C_{\text{mg/L}}^{0.47}$, and that of runoff discharge during the same period is $\phi = 0.048Q_{\text{mcs}}^{0.66}$ (mcs = cubic meters per second). From the double identity $\phi = 0.24C_{\text{mg/L}}^{0.47} = 0.048Q_{\text{mcs}}^{0.66}$, the relationship between $C_{\text{mg/L}}$ and Q can be written as $C_{\text{mg/L}} = 0.032Q_{\text{mcs}}^{1.40}$. This is remarkably close to the equation obtained by regression analysis, $C_{\text{mg/L}} = 0.04Q_{\text{mcs}}^{1.3}$, found in Julien (1995, p. 234). A similar relationship can be defined for the Colorado river at Lee's Ferry from $\phi = 7.5 \times 10^{-4} C_{\text{mg/L}}^{0.88} = 5.25 \times 10^{-4} Q_{\text{ft}^3/\text{s}}^{0.80}$, or $C_{\text{mg/L}} = 0.67Q_{\text{ft}^3/\text{s}}^{0.91}$.

The expected value of variable x can be directly estimated from (9), given the inverse transform parameters \hat{a} and \hat{b}

$$\bar{x} = \left(\frac{1}{a}\right)^{1/b} \Gamma\left(1 + \frac{1}{b}\right) = \hat{a}\Gamma(1 + \hat{b}) = \hat{a}\hat{b} \quad (16)$$

For instance, the mean daily flow of the Chaudière river is calculated directly from the inverse transform parameters by the method of moments in Table 4, thus $\bar{Q} = 98.4\Gamma 2.52 = 98.4!1.52 = 132 \text{ m}^3/\text{s}$.

As a third practical example, the transforms enable very rapid calculations of the sediment discharge of a river once the inverse transform parameters \hat{a} and \hat{b} have been determined. The average sediment load in suspension in the Colorado river at Lee's Ferry (shown in Fig. 12) is estimated from the transform parameters \hat{a} and \hat{b} for Q_s in Table 4. The average daily sediment discharge $\bar{Q}_s = 120,230!1.70 = 185,700$ tons/day calculated from daily measurements over a period of five years (1955–59) is close to the average measurement of 140,000 tons/day for the period 1912–65 calculated by C. F. Nordin Jr. (personal communication, 1995). This approximation based on the transform parameters, circumvents the traditional sediment-load calculations using the combined flow-duration curve and sediment-rating curve method. It should prove particularly useful in rivers with significant washload where sediment concentration and discharge are uncorrelated and the sediment-rating curve is difficult to determine.

As a fourth practical example, the transforms also enable the user to estimate the daily sediment discharge that will be exceeded a certain fraction of the time from (15) after solving for x

$$x = [-\ln P(x)]^{1/b} \left(\frac{1}{a}\right)^{1/b} = \hat{a}[-\ln P(x)]^{\hat{b}} \quad (17)$$

For instance, the daily sediment discharge of the Colorado river at Lee's Ferry that is exceeded 1% of the time, or 3.65 days a year, is calculated with $\hat{a} = 120,230$ and $\hat{b} = 1.7$; $P(Q_s) = 0.01$, which gives $Q_s = 120,230(-\ln 0.01)^{1/1.7} = 1.6 \times 10^6$ tons/day. Conversely, one can estimate the percentage of the time where the daily sediment discharge exceeds a certain value. For instance, how many days a year can someone expect the daily sediment discharge to exceed 1 million tons per day. From (15), one obtains directly $P(Q_s) = e^{-aQ_s^b} = e^{-1.04 \times 10^{-3}(1 \times 10^6)^{1.7}} = 0.027$, or about 10 days per year (0.027×365 days).

NONLINEARITY

The inverse transform exponent \hat{b} is viewed as a measure of nonlinearity between runoff, or sediment transport, and point rainfall. It can be seen from Table 4 that point rainfall is nearly linear with values of $0.85 < \hat{b} < 1.28$. There is a general increase in nonlinearity as depicted by the inverse transform exponent \hat{b} in going from point rainfall to runoff to chemical/sediment transport. The range of values of \hat{b} for various processes is summarized in Table 5. In increasing order

TABLE 5. Typical Values of \hat{b} for Different Variables

| Process (1) | \hat{b} (2) |
|-------------------------------|------------------|
| Point rainfall | 0.85–1.28 |
| Upland snowmelt | 1.15–1.37 |
| Upland chemical concentration | 0.46–1.40 |
| Upland runoff | 1.46–1.62 |
| River flow discharge | 1.25–1.77 |
| River sediment concentration | 1.13–2.14 |
| Upland chemical yield | 1.48–2.33 |
| Upland sediment yield | 2.20–2.35 |
| River sediment discharge | 1.70–2.84 |

of nonlinearity, one finds point rainfall, surface runoff, chemical and sediment concentration, and chemical and sediment yield. The importance of \hat{b} is illustrated with the following analysis and examples.

Once the magnitude x_1 and exceedance probability P_1 of an event are known, one can determine the unknown magnitude x_2 of another event of exceedance probability P_2 simply as a function of the inverse transform exponent \hat{b} . At a given \hat{b} , one defines $\xi = P_2/P_1$ to determine the unknown $\eta = x_2/x_1$. From (15), one obtains $P_1 = e^{-\alpha \hat{b}}$ and $\xi P_1 = e^{-\alpha(\eta x_1)^{\hat{b}}}$ to be solved for ξ as a function of η and b as

$$\xi = e^{-\alpha \hat{b}(\eta^{\hat{b}} - 1)} = P_1^{\eta^{\hat{b}} - 1} \quad (18)$$

or conversely for η as a function of ξ and \hat{b}

$$\eta = \left[1 + \frac{\ln \xi}{\ln P_1} \right]^{\hat{b}} = \left[\frac{\ln P_2}{\ln P_1} \right]^{\hat{b}} \quad (19)$$

which shows that at any given value of ξ and P_1 , the magnitude of η increases with the exponent \hat{b} .

As a fifth example, it is known that in the Colorado river ($\hat{b} = 1.7$) the daily sediment discharge of $x_1 = 1 \times 10^6$ tons/day is exceeded 10 days a year ($P_1 = 0.0274$). Calculate the exceedance probability P_2 of a daily sediment discharge $x_2 = 2 \times 10^6$ tons/day. In this first case, ξ is calculated from (18), given $\eta = x_2/x_1 = 2$ and $b = 1/\hat{b} = 0.59$ for the Colorado river, thus $\xi = (0.0274)^{(2^{0.59} - 1)} = 0.162$ or $P_2 = 0.162 P_1 = 4.45 \times 10^{-3}$ or 1.62 days per year.

As a sixth example, the magnitude of infrequent events can be estimated from the mean value \bar{x} and \hat{b} . For instance, given the mean daily sediment discharge of 185,700 tons/day in the Colorado river ($\hat{b} = 1.7$), estimate the magnitude of the daily sediment discharge x_2 exceeded one day per year ($P_2 = 0.00274$). The exceedance probability of the mean daily sediment discharge of the Colorado river $\bar{Q}_s = 185,700$ tons/day is first calculated from (15) given $a = 1.04 \times 10^{-3}$ and $b = 0.59$. This yields $P_1 = P(\bar{Q}_s) = e^{-1.04 \times 10^{-3} \times 185,700^{0.59}} = 0.263$. The value of η is then calculated from (19), given $\xi = P_2/P_1 = 0.0104$ and $\hat{b} = 1.70$ for the Colorado river, thus $\eta = [1 + (\ln 0.0104 / \ln 0.263)]^{1.7} = 12.5$ or $x_2 = \eta x_1 = 12.5 \times 185,700 = 2.32 \times 10^6$ tons/day. This example shows that the higher the value of \hat{b} associated with nonlinearity, the higher the value of η , and subsequently x_2 .

As a final result, the transforms enable the user to calculate the magnitude of infrequent events from the mean value of a variable and the inverse transform parameter \hat{b} . Considering the previous example, one demonstrates from (9) and (15) that the exceedance probability of the mean value is only a function of \hat{b} as

$$-\ln P(\bar{x}) = (\hat{b})^{1/\hat{b}} \quad (20)$$

The value of x that has an exceedance probability $P(x)$ is then directly calculated from (19) as a function of \bar{x} and \hat{b}

$$x = \left[\frac{\ln P(x)}{\ln P(\bar{x})} \right]^{\hat{b}} \bar{x} = \left[\frac{[-\ln P(x)]^{\hat{b}}}{[-\ln P(\bar{x})]^{\hat{b}}} \right] \bar{x} \quad (21)$$

This equation is quite simple and demonstrates the usefulness of the inverse transform parameter \hat{b} .

As a last practical example, the mean daily sediment concentration in a river is 250 mg/L. Estimate the value of concentration that is exceeded 5% of the time [$P(x) = 0.05$]. Without knowing the distribution of daily sediment-concentration measurements, one can nevertheless find rough estimates from $1.13 < \hat{b} < 2.14$ in Table 5. Hence, one can estimate x assuming $\hat{b} \cong 1.6$ to get from (21), $x = [(-\ln 0.05)^{1.6} / 1.43] \times 250$ mg/L $\cong 1,000$ mg/L. The brackets obtained from $\hat{b} = 1.13$ and $\hat{b} = 2.14$ are, respectively, $x \cong 800$ mg/L and $x \cong 1,150$ mg/L. One would thus expect the daily sediment concentration exceeded 5% of the time to range between 800 and 1,150 mg/L.

SUMMARY AND CONCLUSIONS

This study examines the information contained in rainfall-runoff-transport variables in terms of expected value, duration curves, and exceedance probability. Starting from exponential distribution of rainfall characteristics, the properties of power transforms and the practical implications of the nonlinearities of the transform are examined from point characteristics to runoff and sediment transport in large watersheds.

Transforms are proposed for the analysis of the probability density functions of rainfall, runoff, sediment, and chemical transport variables. Two transform parameters are evaluated either from a graphical method or from the method of moments. The results enable rapid estimates of expected values and exceedance probability at a given value of parameters such as rainfall intensity, duration, depth, flow discharge, chemical concentration, sediment concentration, sediment yield, and sediment discharge.

The transforms are particularly valuable in the analysis of flow and sediment duration curves, as well as for the definition of poorly correlated and sediment-rating curves. In the determination of the mean annual sediment yield in a river, the method circumvents the tedious combined flow-duration curve and sediment-rating curve method. Moreover, the sediment-duration curves can be determined with an assessment of how frequently a daily sediment discharge, or sediment concentration level is exceeded.

The values of the inverse transform exponents \hat{b} are quite representative of physical processes. Point rainfall duration, intensity and depth are nearly exponentially distributed and \hat{b} remains close to unity. Surface runoff discharge and volume per unit area display values of \hat{b} closer to the flow resistance exponent β . The concentration of chemicals in surface runoff varies with values of $0.7 < \hat{b} < 2.2$. Likewise, sediment yield, sediment concentration, and sediment discharge become highly nonlinear and $1.1 < \hat{b} < 2.6$. The value of \hat{b} can be used to estimate the magnitude of infrequent events.

ACKNOWLEDGMENTS

The writer is grateful to C. F. Nordin Jr. for the informative discussion on the sediment load of the Colorado river, and to A. T. Hjelmfelt Jr. for the unpublished report of R. B. Burwell on the plot records from claypan soils in Missouri. Financial support from the Army Research Office (grant ARO/DAAH 04-94-G-0420) is gratefully acknowledged.

APPENDIX I. REFERENCES

- Ashkar, F., and Rousselle, J. (1981). "Design discharge as a random variable: A risk study." *Water Resour. Res.*, 17(3), 577–591.
- Cadavid, L., Obeysekera, J. T. B., and Shen, H. W. (1991). "Flood-frequency derivation from kinematic wave." *J. Hydr. Engrg.*, ASCE, 117(4), 489–509.
- Diaz-Granados, M. A., Valdes, J. B., and Bras, R. L. (1984). "A physically based flood frequency distribution." *Water Resour. Res.*, 20(7), 995–1002.

- Eagleson, P. S. (1972). "Dynamics of flood frequency." *Water Resour. Res.*, 18(2), 878–898.
- Eagleson, P. S. (1978). "Climate, soil and vegetation, 2. The distribution of annual precipitation derived from observed storm sequence." *Water Resour. Res.*, 14(5), 713–721.
- Ferguson, R. I. (1986). "River loads underestimated by rating curves." *Water Resour. Res.*, 22(1), 74–76.
- Fontaine, T. A., and Potter, K. W. (1989). "Estimating probabilities of extreme rainfalls." *J. Hydr. Engrg.*, ASCE, 115(11), 1562–1575.
- Foufoula-Georgiou, E. (1989). "A probabilistic storm transposition approach for estimating exceedance probabilities of extreme precipitation depths." *Water Resour. Res.*, 25(5), 799–815.
- Govindaraju, R. S., and Kavvas, M. L. (1991). "Stochastic overland flows, Part 2: Numerical solutions evolutionary probability density functions." *Stochastic Hydro. and Hydr.*, 5, 105–124.
- Gumbel, E. J. (1958). *Statistics of extremes*. Columbia University Press, New York, N.Y.
- Hawkins, R. H. (1993). "A symptotic determination of runoff curve numbers from data." *J. Irrig. and Drain. Engrg.*, ASCE, 119(2), 334–345.
- Hebson, C., and Wood, E. F. (1982). "A derived flood frequency distribution using Horton order ratios." *Water Resour. Res.*, 18(5), 1509–1518.
- Hjelmfelt, A. T. (1991). "Investigation of curve number procedure." *J. Hydr. Engrg.*, ASCE, 117(6), 725–737.
- Hjelmfelt, A. T., and Burwell, R. E. (1984). "Spatial variability of surface runoff." *J. Irrig. and Drain. Engrg.*, ASCE, 110(1), 46–54.
- Jamison, V. C., Smith, D. D., and Thornton, J. F. (1968). "Soil and water research on a claypan soil." *USDA, ARS, Tech. Bull. No. 1379*, U.S. Govt. Printing Ofc., Washington, D.C.
- Johnson, H. P., and Baker, J. L. (1982). "Field-to-stream transport of agricultural chemicals and sediment in an Iowa watershed part I: Data base for model testing (1976–1978)." *Rep. EPA-600/3-82-032*, Envir. Res. Lab., Envir. Protection Agency (EPA), Athens, Ga.
- Julien, P. Y. (1982). "Prédiction d'apport solide pluvial et nival dans les cours d'eau nordiques à partir du ruissellement superficiel," PhD dissertation, Civ. Engrg. Dept., Laval Univ., Québec, Canada (in French).
- Julien, P. Y. (1995). *Erosion and sedimentation*. Cambridge University Press, London, England.
- Julien, P. Y., and Frenette, M. (1985). "Modeling of rainfall erosion." *J. Hydr. Engrg.*, ASCE, 111(10), 1344–1359.
- Julien, P. Y., and Moglen, G. E. (1990). "Similarity and length scale for spatially-varied overland flow." *Water Resour. Res.*, 26(8), 1819–1832.
- Kavvas, M. L., and Govindaraju, R. S. (1991). "Stochastic overland flows Part 1: Physics-based evolutionary probability distributions." *Stochastic Hydro. and Hydr.*, 5, 89–104.
- Moughamian, M. S., McLaughlin, D. B., and Bras, R. L. (1987). "Estimation of flood frequency: an evaluation of two derived procedures." *Water Resour. Res.*, 23(7), 1309–1319.
- Nguyen, V. T. V., and Rousselle, J. (1981). "A stochastic model for the time distribution of hourly rainfall depth." *Water Resour. Res.*, 17(2), 399–409.
- Ogden, F. L., and Julien, P. Y. (1993). "Runoff sensitivity to temporal and spatial rainfall variability at runoff plan and small basin scale." *Water Resour. Res.*, 29(8), 2589–2597.
- Ogden, F. L., Richardson, J. R., and Julien, P. Y. (1995). "Similarity in catchment response 2. moving rainstorms." *Water Resour. Res.*, 31(6), 1543–1547.
- Raines, T., and Valdes, J. B. (1993). "Estimation of flood frequencies for ungaged catchments." *J. Hydr. Engrg.*, ASCE, 119(10), 1138–1154.
- Rousseau, C. (1979). "Analyse des caracteristiques hydrologiques d'une couverture nivale." MS thesis, Civ. Engrg. Dept., Laval Univ., Québec, Canada (in French).
- Saghafian, B., Julien, P. Y., and Ogden, F. (1995). "Similarity in catchment response 1. stationary rainstorms." *Water Resour. Res.*, 31(6), 1533–1541.
- Schaake, J. C., Geyer, J. C., and Knapp, J. W. (1967). "Experimental examination of the rational method." *J. Hydr. Engrg.*, ASCE, 93(6), 353–370.
- Shen, H. W., Koch, G. J., and Obeysekera, J. T. B. (1990). "Physically based flood features and frequencies." *J. Hydr. Engrg.*, ASCE, 116(4), 494–514.
- Smith, C. N., Leonard, R. A., Langdale, G. W., and Bailey, G. W. (1978). "Transport of agricultural chemicals from small upland piedmont watersheds." *Rep. EPA-600/3-78-056*, U.S. Envir. Protection Agency (EPA), Athens, Ga.
- Stedinger, J. R., Vogel, R. M., and Foufoula-Georgiou, E. (1993). "Chapter 18: Frequency analysis of extreme events." *Handbook of hydrology*, McGraw-Hill, New York, N.Y.
- Todorovic, P. (1968). "A mathematical study of precipitation phenomena." *Rep. CER67-68PT65*, Engrg. Res. Ctr., Colorado State Univ., Fort Collins, Colo.
- Todorovic, P., and Rousselle, J. (1971). "Some problems of flood analysis." *Water Resour. Res.*, 7(5), 1144–1150.
- Todorovic, P., and Woolhiser, D. A. (1974). "Stochastic model of daily rainfall." *Proc., Symp. on Statistical Hydro., Misc. Publ. No. 1275*, U.S. Dept. of Agric., Agric. Res. Service, 232–246.
- Villeneuve, G. O. (1968). "Données météorologiques de la station agronomique de Laval." *Data Rep. Publ. MP-9, MP-17, MP-23, MP-33, and MP-52 for 1966, 1967, 1968, 1969, 1970*, Publ. MP-9, Ministère des Richesses Naturelles, Québec, Canada (in French).
- Wood, E. F., and Hebson, C. S. (1986). "On hydrologic similarity. 1. Derivation of the dimensionless flood frequency curve." *Water Resour. Res.*, 21(11), 1549–1554.
- Woolhiser, D. A. (1975). "Chapter 12: Simulation of unsteady overland flow." *Unsteady flow in open channels*, Water Resources Publications, Littleton, Colo., 485–508.
- Woolhiser, D. A. (1977). "Unsteady free-surface flow problems." *Mathematical models for surface water hydrology*, John Wiley & Sons, New York, N.Y., 195–213.

APPENDIX II. NOTATION

The following symbols are used in this paper:

- a, b = transform coefficient and exponent;
 \hat{a}, \hat{b} = inverse transform coefficient and exponent;
 C = Chézy coefficient;
 $C_{mg/L}$ = sediment concentration in mg/L;
 f = Darcy-Weisbach friction factor;
 g = gravitational acceleration;
 h = flow depth;
 i = rainfall intensity;
 K = laminar resistance coefficient;
 L = runoff length;
 M_1, M_2 = first and second moments of distribution;
 n = Manning resistance coefficient;
 $P(\phi)$ = exceedance probability, $P(\phi) = \int_{\phi}^{\infty} p(\xi) d\xi$;
 $p(\phi)$ = probability density function;
 Q = total discharge;
 Q_s = daily sediment discharge;
 q = unit discharge;
 S = friction slope;
 t = time;
 t_e = time to equilibrium;
 t_r = rainfall duration;
 x, \bar{x}, y = variables;
 \bar{x} = average value of x ;
 α, β = coefficient and exponent of resistance relationship;
 $\Gamma(x + 1)$ = gamma function, $\Gamma(x + 1) = !x$;
 θ = dimensionless time, $\theta = (t - t_r)/t_e$;
 λ = dimensionless time ratio, $\lambda = t_r/t_e$;
 λ_1, λ_2 = reciprocal of average rainstorm duration and intensity;
 ν = kinematic fluid viscosity;
 Π = double natural logarithm of $P(\phi)$, $\Pi = \ln[-\ln P(\phi)]$;
 ϕ = reduced variable;
 ψ = dimensionless discharge, $\psi = q/iL$; and
 $!(x)$ = factorial function of x , $!x = x(x - 1)(x - 2) \dots$